ISSN 0869-5911, Petrology, 2018, Vol. 26, No. 2, pp. 115–120. © Pleiades Publishing, Ltd., 2018.
Original Russian Text © L.Ya. Aranovich, N.S. Bortnikov, 2018, published in Petrologiya, 2018, Vol. 26, No. 2, pp. 109–115.

New Zr–Hf Geothermometer for Magmatic Zircons

L. Ya. Aranovich* and N. S. Bortnikov

Institute of the Geology of Ore Deposits, Petrography, Mineralogy, and Geochemistry (IGEM), Russian Academy of Sciences, Moscow, 119017 Russia

**e-mail: lyaranov@igem.ru*

Received May 22, 2017; in final form, September 10, 2017

Abstract—A geothermometer equation $T = \frac{1531}{\ln K_d + 0.883}$, where $K_d = \frac{X^s_{Zr} X^m_{Hf}}{X^m_{Zr} X^s_{Hf}}$ [X^i_j is the concentration (in ppm) of component i in phase j] is the Zr and Hf distribution coefficient between melt and zircon, and T is temperature in K, was derived by thermodynamic processing of literature experimental data on Zr and Hf distribution between acid melts (m) and zircon (s) and on the solubility of zircon and hafnon in the melts with variable silica content. In calculations with this equations, we assumed the Zr concentration in zircon to be constant: 480000 ppm. It is shown that the commonly observed increase in Hf concentration from the cores to margins of magmatic zircon crystals is caused by the fractional crystallization of zircon. For differentiated acid magmatic series, the initial crystallization temperature of zircon in the least silicic cumulates should be evaluated using the cores of large zircon grains with the highest Zr/Hf ratio. Application of the geothermometer for mafic and intermediate rocks may be hampered due to simultaneous crystallization of zircon with some other ore and mafic minerals relatively enriched in Zr and Hf. The newly derived geothermometer has some advantages over other indicators of the crystallization temperature of magmatic zircon based on the zircon saturation index (Watson and Harrison, 1983; Boehnke et al., 2013) and on Ti concentration in this mineral (Ferry and Watson, 2007) as it does not depend on the major-oxide melt composition and on the accuracy of the estimated SiO_2 and TiO_2 activities in the melts. Calculations of the Zr and Hf fractionation trends in the course of zircon crystallization in granitoid melts allow one to evaluate the temperature at which more evolved melt portions were segregated.

DOI: 10.1134/S0869591118020029

INTRODUCTION

Magmatic zircon commonly contains from 0.5 to 5 wt % HfO_2 (Hoskin and Schaltegger, 2003, and references therein), i.e., is a solid solution of zircon (*Zrn*, $ZrSiO_4$) and hafnon (*Hfn*, $HfSiO_4$). The literature provides descriptions of numerous documented instances when the Zr/Hf ratio decreases from the cores to margins of individual magmatic zircon grains (Claiborne et al., 2006, 2010; Wang et al., 2010; Padilla et al., 2016; Aranovich et al., 2017), as well as from more mafic to more silicic rocks in differentiated continental magmatic series (Barth and Wooden, 2010; Claiborne et al., 2006; 2010; Padilla et al., 2016). A negative correlation between the Zr/Hf ratio and Ti concentration in zircon, which is an indicator (at least qualitative) of the crystallization temperature of this mineral (Ferry and Watson, 2007), was determined in (Barth and Wooden, 2010; Claiborne et al., 2006, 2010; Grimes et al., 2009). These relations seem to be paradoxical because Zr and Hf are elements of very similar crystal chemical properties (the formal charge is +4, and ionic radii in the eight-fold coordination are 0.83 and 0.84 Å, respectively; Shannon, 1976), and hence, these elements should be weakly fractionated during deep petrogenetic processes (Taylor and McLennan, 1985). These relations become, however, understandable considering the fact that the most compatible element in zircon during its crystallization from a magmatic melt is Zr itself, i.e., the exchange reaction

$$HfSiO_4 + ZrSiO_4^m = ZrSiO_4 + HfSiO_4^m, \qquad (1)$$

where m is silicate melt, is notably shifted to the right. This follows from experimental data on zircon and hafnon solubility in silicate melts (Ellison and Hess, 1986; Linnen and Kepler, 2002) and on Zr and Hf distribution between zircon and melt (Rubatto and Hermann, 2007), as well as from theoretical estimates of the Zr and Hf partition coefficients in the system zircon–silicate melt on the basis of the lattice strain model (Blundy and Wood, 2003). The temperature dependence of Zr and Hf distribution between zircon and silicate melt have never been studied before and is discussed below.

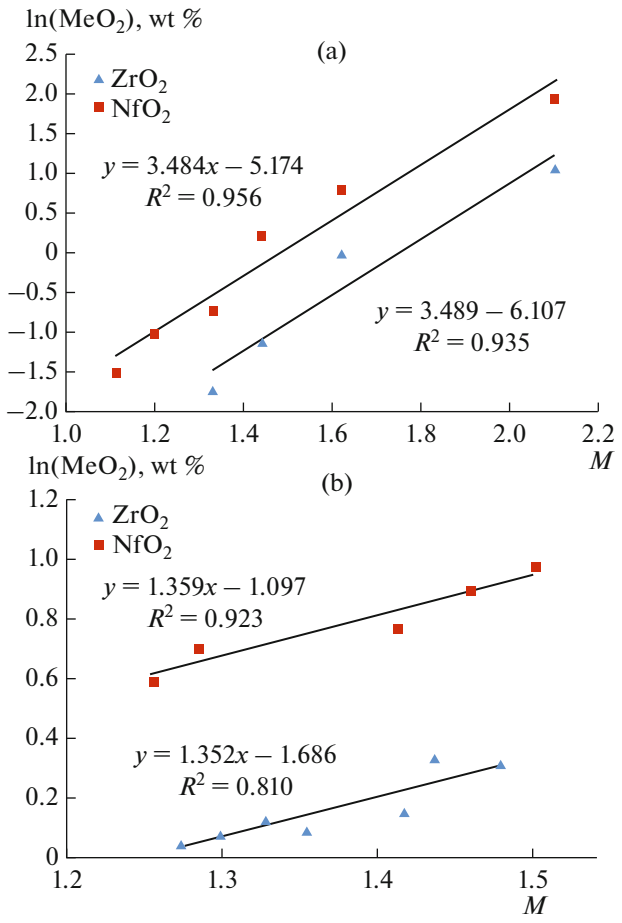

Fig. 1. Dependence of the ZrO_2 (triangles) and HfO_2 (squares) concentrations (wt %) on the composition of melts saturated with zircon and hafnon, respectively. (a) 800°C, according to (Linnen and Keppler, 2002); (b) 1400°C, according to (Ellison and Hess, 1986). The figure shows the linear regression equation and correlation coefficients.

THERMODYNAMIC RELATIONS

The equilibrium conditions of exchange reaction (1) are written as

$$RT\ln K(1) + \Delta G^\circ(1) = 0, \quad (2)$$

where $R = 8.314$ J/(mol K) is the universal gas constant, T is the absolute temperature, K, $K(1)$ is the reaction constant (activity product), and $\Delta G^\circ(1)$ is the standard Gibbs free energy of reaction (1), J/mol.

The reaction constant can be expressed as

$$K(1) = \frac{X^s_{Zr}X^m_{Hf}}{X^m_{Zr}X^s_{Hf}}\frac{\gamma^s_{Zr}\gamma^m_{Hf}}{\gamma^m_{Zr}\gamma^s_{Hf}} = K_d K_\gamma, \quad (3)$$

where $K_d = \frac{X^s_{Zr}X^m_{Hf}}{X^m_{Zr}X^s_{Hf}}$ is the Zr and Hf distribution coefficient between *Zrn*(*s*) and melt, X^j_i is the mole fraction of component i in phase j, K_γ is the product of activity coefficients γ^j_i of the corresponding species.

Because the crystal chemical properties of Zr and Hf are very closely similar, it is reasonable to suggest that the *Zrn*–*Hfn* solution is close to an ideal one. Even if it is not the case, within the narrow range of Hf concentration typical of natural magmatic zircon, in the regular solution approximation, the difference (at T = const)

$$RT(\ln\gamma^s_{Zrn} - \ln\gamma^s_{Hfn}) = W(X^s_{Hf} - X^s_{Zr}) \approx \text{const}, \quad (4)$$

i.e., the term responsible for the nonideality of the *Zrn*–*Hfn* solution is a merely small correction for the $\Delta G^\circ(1)$ value.

The activity coefficients of *Zrn* and *Hfn* in silicate melts, on the contrary, should be notably different from unity. This is evident from the strong dependence of the solubility of the zircon and hafnon end members on the composition of the melt (Figs. 1a, 1b). In constructing the diagram in Fig. 1, we used the melt parameter $M = (Na + K + 2Ca)/(Al \times Si)$, where symbols of elements denote their molar amounts in the melt normalized to the sum of all molar amounts (Watson and Harrison, 1983; Boehnke et al., 2013). These researchers have demonstrated that the empirical parameter M is best suitable for describing the solubility of zircon, i.e., well reflects variations in the thermodynamic properties of zircon in acid melts. As seen in Fig. 1a, the solubility of zircon and hafnon increases by almost one order of magnitude as M increases from 1 to 2. Therewith the slope of the line $d(\ln[MeO_2])/dM$ for both ZrO_2 and HfO_2 is nearly the same at any given T value (Fig. 1), which suggests that the activity coefficients of zircon and hafnon is silicate melts are very similar. Hence, it can be provisionally assumed that the ratio $\frac{\gamma^m_{Hf}}{\gamma^m_{Zr}} = 1$. With regard for (3) and (4), Eq. (2) is then simplified to

$$RT\ln K_d + \Delta G^{\circ *}(1) = 0, \quad (5)$$

where $\Delta G^{\circ *}(1)$ may differ, according to (4), from the thermochemical value of $\Delta G^\circ(1)$ by a small value.

To calibrate the temperature dependence of $\Delta G^{\circ *}(1)$ we used experimental data on Zr and Hf distribution between granite melt and zircon (Rubatto and Hermann, 2007), which were processed with Eq. (5), and results of experiments on zircon and hafnon solubility in melts of various composition (Ellison and Hess, 1986; Linnen and Kepler, 2002). If the dissolution of minerals is expressed as the schematic reactions

$$(HfSiO_4)^s = (HfSiO_4)^m, \quad (6)$$

$$(ZrSiO_4)^s = (ZrSiO_4)^m, \quad (7)$$

then at any given T, P, and melt composition M and with regard for $\frac{\gamma^m_{Hf}}{\gamma^m_{Zr}} = 1$, we arrive at

$$\Delta G^{\circ *}(1) = \Delta G^{\circ *}(6) - \Delta G^{\circ *}(7) = RT\ln(X_{Zr}/X_{Hf})^m. \quad (8)$$

The values used to determine the temperature dependence of $\Delta G^{\circ *}(1)$ are given in Table 1 and shown in Fig. 2. For experiments at a constant temperature but different M of the melt (Ellison and Hess, 1986; Linnen and Kepler, 2002), Table 1 lists average $\Delta G^{\circ *}(1)$ values. As seen in Fig. 2, the linear equation

$$\Delta G^{\circ *}(1) = -12726 + 7.34T \quad (9)$$

well fits all experimental data within their errors, which were estimated for $\Delta G^{\circ *}(1)$ at approximately ±500–700 J based on the probable analytical errors (7–10 relative %) of ZrO_2 and HfO_2 concentrations in the experimental melts (Ellison and Hess, 1986; Rubatto and Hermann, 2007; Linnen and Keppler, 2002).

Substituting Eq. (9) in (5), we arrive at the following simple expression for the Zr–Hf geothermometer for zircon-bearing magmatic rocks:

$$T = \frac{1531}{\ln K_d + 0.883}. \quad (10)$$

As an illustrative example, Table 2 lists temperature estimates with the geothermometer [Eq. (10)] for samples from the Austurhorn magmatic complex, Iceland, which is described in much detail in (Padilla et al., 2016). In calculating the Zr/Hf ratio, we assumed that Zr concentration in the zircon is constant: [Zr] = 480000 ppm. The calculation results are presented in Table 2, together with temperature estimates obtained in (Padilla et al., 2016) using the zircon saturation index according to (Boehnke et al., 2013). For rocks relatively rich in silica (sample with *NS* index in Table 2), the agreement between temperature estimates by the two methods is reasonably good, but for the gabbroic samples (labeled *G* in Table 2) calculations with the zircon saturation index yield unrealistically low values. The reason for these discrepancies is quite obvious: the bulk composition of mafic rocks does not correspond to the composition of the melt from which the zircons actually crystallized during the late differentiation stages of the melts, and this leads to significant underestimates of the temperature values based on the zircon saturation index. It is also quite probable that appreciable amounts of Zr and Hf could be accommodated in rock-forming magmatic minerals (such as clinopyroxene and amphibole) and in certain accessories (sphene and ilmenite) during the crystallization of the gabbro (Bea et al., 2006), and hence, the bulk-rock Zr/Hf ratio of the rock might differ from that of the melt from which the zircon started to crystallize.

FRACTIONAL CRYSTALLIZATION OF ZIRCON

According to Eqs. (5) and (9), the lower the temperature, the greater the difference between the Zr/Hf ratios of silicate melt and zircon. At a constant Zr/Hf ratio in the melt, zircon crystallizing from this melt on cooling should have been progressively depleted in Hf. However, relations detected in nature are usually just opposite: Hf concentration increases from zircon cores to margins (Fig. 3; see also Claiborne et al., 2006; 2010; Aranovich et al. 2017). The obvious reason for this is a decrease in the Zr/Hf ratio in the melt in the course of fractional crystallization of zircon, a process that can be described by the Rayleigh fractionation equation

$$C^m = C^{0,m} \times f^{(K_d-1)}, \quad (11)$$

where C^m and $C^{0,m}$ are the current and starting Zr/Hf ratios of the melt, and f is the fraction of melt from which the zircon crystallizes, $0 \le f \le 1$. Note that the value of f not always reflects the actual crystallinity of silicate melts but only the beginning (at $f = 1$) and end (at $f = 0$) of zircon crystallization. Zircon starts to crystallize when its saturation index has been reached,

Table 1. Data used to calculate the temperature dependence of $\Delta G^{\circ *}(1)$

T, K	$\Delta G^{\circ *}(1)$	Reference[#]	Equation[##]
1073.15	−423	1	5
1173.15	−3547	1	5
1223.15	−3440	1	5
1273.15	−3201	1	5
1323.15	−3054	1	5
1073.15	−5480[$]	2	8
1308.15	−3990[$]	2	8
1673.15	−338[$]	3	8

[#] Sources of experimental data: (1) (Rubatto and Hermann, 2007); (2) (Linnen and Keppler, 2002); (3) (Ellison and Hess, 1986).[##] Number of equation (see text) used in the calculations. [$] Average of values calculated for experiments with melts of various M at corresponding temperature.

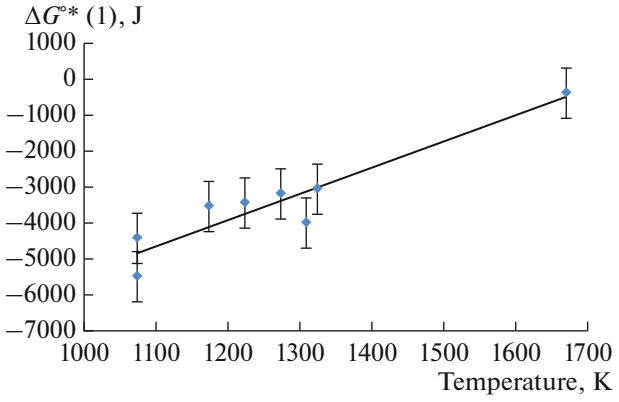

Fig. 2. Dependence of the Gibbs free energy of exchange reaction (1) on absolute temperature. Diamonds with error brackets are experimental data (see Table 1), and the solid line is a linear approximation.

Table 2. Comparison of temperature estimates by the Zr–Hf geothermometer [Eq. (10) in text, *T*, °C (10)] and using the zircon saturation index (*Zrn*–*T*, °C)

Number of *Zrn* grain	Zr/Hf, rock	Zr/Hf, *Zrn*	*T*, °C (10)	*Zrn*–*T*, °C
IA-NS-2-4.1	33.01	57.83	787	846
IA-NS-6-2.1	39.48	66.67	815	766
IA-NS-7-15.1	43.41	78.30	766	904
IA-G-1-26.1	35.26	58.14	833	535
IA-G-5-10.1	37.70	73.64	713	564

Sample numbers and analytical data are according to (Padilla et al., 2016; Tables S1 and S3). The calculation of *Zrn*-*T*, °C in (Padilla et al., 2016; Table S1) was conducted using (Boehnke et al., 2013).

which depends on the starting Zr concentration, the SiO_2 concentration/activity in the melt, and the composition of the melt, which is expressed by the *M* index (Watson and Harrison, 1983; Boehnke et al., 2013).

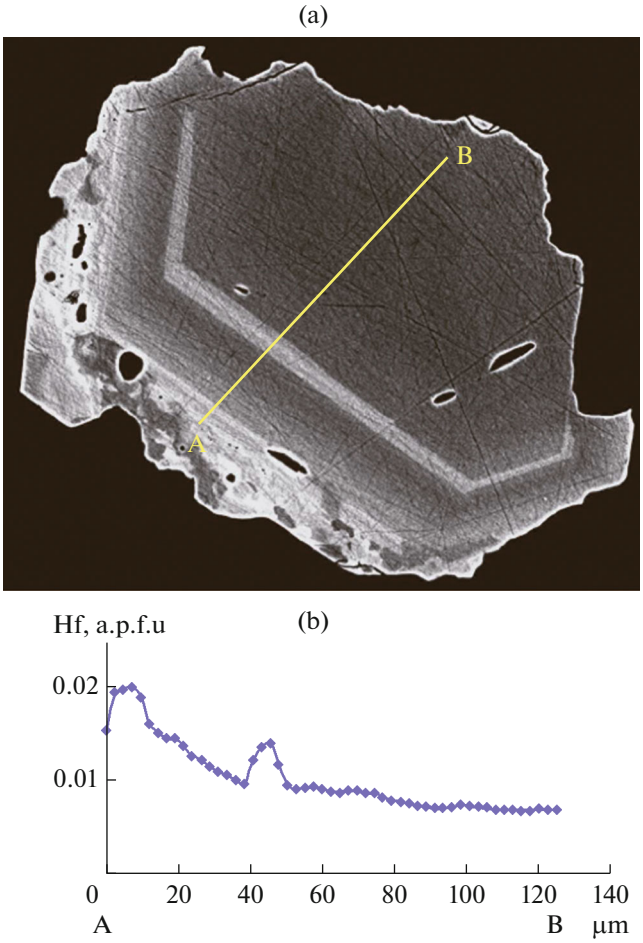

Fig. 3. (a) BSE image and (b) variations in Hf concentration (a.p.f.u.) along profile A–B, according to (Aranovich et al., 2017).

Because of this, zircon is one of the first phases to crystallize in granites (at least those of normal alkalinity), but in mafic melts, this mineral commonly crystallizes during their late differentiation, when the true melt fraction is much lower than one. Conversely, zircon crystallization can terminate because of Zr depletion before the complete crystallization of the melt, i.e., when the true melt fraction is greater than zero.

An example of calculations with Eq. (11) is shown in Fig. 4 . The starting value of $C^{0,m}$ is taken according to analytical data (Claiborne et al., 2010, Table 1) for a cumulus rock sample BC101-Z (70.84 wt % SiO_2) from the Spirit Mountain granite batholith, Nevada: $C^{0,m}$ =39.55. Zircons from this sample show significant variations in Hf concentration and, accordingly, in the Zr/Hf ratio (Claiborne et al., 2010, Table 3). The initial K_d value in Eq. (11) was calculated using the highest $(Zr/Hf)^{Zrn} = 65.7$, which was measured in the core of grain BC101-2.2C (Claiborne et al., 2010, Table 3). The temperature calculated by Eq. (10) for the beginning of zircon crystallization ($f = 1$), T_0 = 828°C, is only 14°C lower than the temperature estimate based on the Ti concentration in the zircon as given in (Claiborne et al., 2010, Table 3). The agreement between the values is very good, with regard for the calibration errors of both thermometers, analytical errors, and uncertainties in the SiO_2 and TiO_2 activities in the expression for the Ti-in-*Zrn* geothermometer (see discussion in Aranovich et al., 2013). The composition trends of the melt and zircon (solid lines in Fig. 3) were calculated under the assumption that the melt fraction *f* is a linear function of temperature

$$f = 1 - k(T - T_0), \quad (12)$$

and the coefficient $k = 0.0067$ was determined under the assumption that $f = 0$ at a temperature T_{fin} = 680°C, which corresponds to the solidus of hydrous granite under a pressure of 2 kbar (Ebadi and Johannes, 1991). If the dependence $f(T)$ is logarithmic at the same T_0 and T_{fin} values, the position of curves in Fig. 4 practically does not change. Since the value of T_0 is constant, the location of the fractionation curves depends mostly on the value of k, which, in turn, depends on $T_{fin.}$ At T_{fin} = 730°C (granite solidus at a pressure of 1 kbar; Ebadi and Johannes, 1991) (k = 0.01), the composition trends of both phases become steeper (dashed lines in Fig. 4), and at T_{fin} = 650°C (granite solidus under a pressure of 3–4 kbar; Ebadi and Johannes, 1991) and k = 0.0056, the slopes are gentler (dotted lines in Fig. 4). Because the value of *f* for granite melts roughly corresponds to the actual melt fraction, calculating curves analogous to those in Fig. 4 allows one to estimate the final crystallization temperature of zircon, and for the differentiated series, also the temperature at which evolved melts were segregated. For the above example of the Spirit Mountain batholith, the lowest ratio Zr/Hf = 32.5 was found in the zircon grain BC101-7.2R from the cumulus rock of

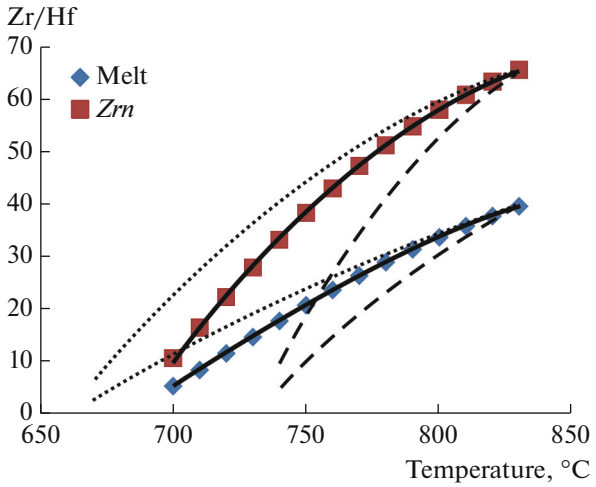

Fig. 4. Trends in the variations in the Zr/Hf ratio of zircon (squares) and melt (diamonds) during the fractional crystallization of zircon from granitoid melt (analytical data on the composition of rock and zircon of sample BC101-Z; Claiborne et al., 2010): calculation by Eq. (11) (see text) at an initial crystallization temperature of zircon $T_0 = 830$°C and its final crystallization temperatures $T_{fin} = 680$ (solid lines), 730 (dashed lines), and 650°C (dotted lines).

sample BC101 (Claiborne et al., 2010, Table 3). Depending on the selected k value, this composition corresponds to a final temperature of zircon crystallization within the range of 725–760°C. In leucogranites, which are the most evolved melt portions segregated from the main chamber, Zr/Hf = 23.57 and 20.46 (samples SML49Z and LGZ, respectively; Claiborne et al., 2010, Table 1). Melt differentiation curves in Fig. 3 suggest that the melts were segregated at temperatures of 730–780°C, and the most realistic temperature range seems to be 740–760°C (curves at $T_{fin} = 680$°C, $k = 0.0067$). The melt fraction was then around 0.4–0.5.

CONCLUSIONS

Because of its refractory nature and very low values of the diffusion coefficients of tetravalent cations (Cherniak et al., 1997; Cherniak and Watson, 2003), which minimize the intracrystalline diffusion-controlled redistribution of isomorphic components, zircon is one of the most efficient monitors of the evolution of magmatic processes. The distribution of Zr and Hf between zircon and silicate melt is a sensitive function of the crystallization temperature of the mineral, and often observed Hf zoning in magmatic zircon results from the zircon growth during fractional crystallization of the melt. As a result of this process, the Zr/Hf ratio should decrease from the cores to margins of the zircon crystals. The Zr/Hf ratio of the melt also decreases, and consequently, the cores of zircon grains crystallizing later in the course of magmatic evolution should have lower Zr/Hf ratios. Hence, to estimate the starting crystallization temperature of zircon with the Zr–Hf geothermometer the composition of the cores of the largest grains with the maximum Zr/Hf ratio should be used. When using the newly derived geothermometer in application to mafic magmatic rocks, one should be aware of the fact that the bulk Zr/Hf ratio of the rock may not reflect the composition of the melt when zircon started to crystallize because of the preceding or simultaneous crystallization of certain rock-forming, minor, and accessory minerals.

In calculating the fractionation curves (Fig. 4), we assumed that the only solid phase containing Zr and Hf was zircon. The presence of other magmatic minerals able to accumulate appreciable amounts of these elements, as well as peritectic reactions between these minerals and melt during magmatic evolution, can significantly modify the Zr–Hf fractionation trends of the melt (as well as the zircon itself) and even disturb the "regular" Zr–Hf growth zoning pattern of zircon (with Hf concentration increasing toward the margins). The crystallization of such a mineral (most likely, amphibole) may have caused a local Hf maximum in the concentration profile shown in Fig. 3. It is still hardly possible to quantify the contribution of these effects because of the absence of experimental data on the temperature dependence of Zr and Hf distribution between zircon and mafic minerals. These phenomena should most significantly affect temperature estimates for mafic rocks. Further experimental studies are needed to solve this problem. Parameters of Eq. (10) for the geothermometer should also be refined based on experimental data on the solubility of zircon and hafnon in silicate melts within broad temperature and composition ranges.

In spite of the foregoing remarks, the new geothermometer suggested herein has certain advantages over other indicators of crystallization temperature of zircon that are based on the zircon saturation index (Watson and Harrison, 1983; Boehnke et al., 2013) and on Ti concentration in this mineral (Ferry and Watson, 2007). Our geothermometer does not depend on the composition of the melt and on estimates of its SiO_2 and TiO_2 activities. Moreover, reconstructions of Zr and Hf fractionation trends during zircon crystallization from granitoid melts allows one to evaluate the temperature at which more evolved melt portions were segregated.

ACKNOWLEDGMENTS

Critical comments by A.A. Borisov (Institute of the Geology of Ore Deposits, Petrography, Mineralogy, and Geochemistry, Russian Academy of Sciences) allowed us to significantly improve the manuscript. This study is a part of the Russian Science Foundation project no. 18-17-00126.

REFERENCES

Aranovich, L.Ya., Bortnikov, N. S., Zinger, T. F., et al., "Morphology and impurity elements of zircon in the oceanic lithosphere at the Mid-Atlantic Ridge axial zone (6°–13° N): evidence of specifics of magmatic crystallization and postmagmatic transformations, *Petrology,* 2017, vol. 25, no. 4, pp. 339–364.

Aranovich, L.Ya., Zinger, T.F., Bortnikov, N.S., et al., Zircon in gabbroids from the axial zone of the Mid-Atlantic Ridge, Markov Deep, 6 N: correlation of geochemical features with petrogenetic processes, *Petrology,* 2013, vol. 21, no. 1, pp. 1–15.

Barth, A.P. and Wooden, J.L., Coupled elemental and isotopic analyses of polygenetic zircons from granitic rocks by ion microprobe, with implications for melt evolution and the sources of granitic magmas, *Chem. Geol.,* 2010, vol. 277, pp. 149–159.

Bea, F., Montero, P., and Ortega, M., A LA-ICPMS evaluation of Zr reservoirs in common crustal rocks: implications for zircon-forming processes, *Can. Mineral.,* 2006, vol. 44, pp. 745–766.

Blundy, J. and Wood, B., Mineral–melt partitioning of uranium, thorium and their daughters, *Rev. Mineral. Geochem.,* 2003, vol. 52, pp. 59–124.

Boehnke, P., Watson, E.B., Trail, D., et al., Zircon saturation revisited, *Chem. Geol.,* 2013, vol. 351, pp. 324–334.

Cherniak, D.J., Hanchar, J.M., and Watson, E.B., Diffusion of tetravalent cations in zircon, *Contrib. Mineral. Petrol.,* 1997, vol. 127, pp. 383–390.

Cherniak, D.J. and Watson, E.B., Diffusion in zircon, in *Zircon*, Hanchar J.M. and Hoskin P.W.O., Eds., *Rev. Mineral. Geochem.,* 2003, vol. 53, pp. 113–143.

Claiborne, L.L., Miller, C.F., Walker, B.A., et al., Tracking magmatic processes through Zr/Hf ratios in rocks and Hf and Ti zoning in zircons: an example from the Spirit Mountain batholith, Nevada, *Mineral. Mag.,* 2006, vol. 70, pp. 517–543.

Claiborne, L.L., Miller, C.F., and Wooden, J.L., Trace element composition of igneous zircon: a thermal and compositional record of the accumulation and evolution of a large silicic batholith, Spirit Mountain, Nevada, *Contrib. Mineral. Petrol.,* 2010, vol. 160, pp. 511–531.

Ebadi, A. and Johannes, W., Beginning of melting and composition of first melts in the system *Qz–Ab–Or*–H_2O–CO_2, *Contrib. Mineral. Petrol.,* 1991, vol. 106, pp. 286–295.

Ellison, A.J. and Hess, P.C., Solution behavior of +4 cations in high silica melts: petrologic and geochemical implications, *Contrib. Mineral. Petrol.,* 1986, vol. 94, pp. 343–351.

Ferry, J.M. and Watson, E.B., New thermodynamic models and revised calibrations for the Ti-in-zircon and Zr-in-rutile thermometers, *Contrib. Mineral. Petrol.,* 2007, vol. 154, pp. 429–437.

Grimes, C.B., John, B.E., Cheadle, M.J., et al., On the occurrence, trace element geochemistry, and crystallization history of zircon from in situ ocean lithosphere, *Contrib. Mineral. Petrol.,* 2009, vol. 158, pp. 757–783.

Hoskin, P.W.O. and Schaltegger, U., The composition of zircon and igneous and metamorphic petrogenesis, in *Zircon,* Hanchar, J.M. and Hoskin, P.W.O., Eds., *Rev. Mineral. Geochem.,* 2003, vol. 53, pp. 27–62.

Linnen, R.L. and Keppler, H., Melt composition control of Zr/Hf fractionation in magmatic processes, *Geochim. Cosmochim. Acta,* 2002, vol. 66, pp. 3293–3301.

Padilla, A.J., Miller, C.F., Carley, T.L., et al., Elucidating the magmatic history of the Austurhorn silicic intrusive complex (southeast Iceland) using zircon elemental and isotopic geochemistry and geochronology, *Contrib. Mineral. Petrol.,* 2016, vol. 171, p. 69. doi 10.1007/s00410–016–1279-z

Rubatto, D. and Hermann, J., Experimental zircon/melt and zircon/garnet trace element partitioning and implications for the geochronology of crustal rocks, *Chem. Geol.,* 2007, vol. 241, pp. 38–61.

Shannon, R.D., Revised effective ionic radii and systematic studies of interatomic distances in halides and chalcogenides, *Acta Crystal,* 1976, vol. A32, pp. 751–767.

Taylor, S.R. and McLennan, S.M., *The Continental Crust: Its Composition and Evolution*, London: Blackwell, 1985.

Wang, X., Griffin, W.L., and Chen, J., Hf contents and Zr/Hf ratios in granitic zircons, *Geochem. J.,* 2010, vol. 44, pp. 65–72.

Watson, E.B. and Harrison, T.M., Zircon saturation revisited: temperature and composition effects in a variety of crustal magma types, *Earth Planet. Sci. Lett.,* 1983, vol. 64, pp. 295–304.

Translated by E. Kurdyukov